Three metal ions at the active site of the *Tetrahymena* group I ribozyme

Shu-ou Shan*, Aiichiro Yoshida†, Sengen Sun†, Joseph A. Piccirilli†§, and Daniel Herschlag*§

*Department of Biochemistry, Stanford University, Stanford, CA 94305-5307; and †Departments of Biochemistry and Molecular Biology and Chemistry, University of Chicago, Chicago, IL 60637

Communicated by Olke C. Uhlenbeck, University of Colorado, Boulder, CO, August 27, 1999 (received for review May 13, 1999)

Metal ions are critical for catalysis by many RNA and protein enzymes. To understand how these enzymes use metal ions for catalysis, it is crucial to determine how many metal ions are positioned at the active site. We report here an approach, combining atomic mutagenesis with quantitative determination of metal ion affinities, that allows individual metal ions to be distinguished. Using this approach, we show that at the active site of the *Tetrahymena* group I ribozyme the previously identified metal ion interactions with three substrate atoms, the 3′-oxygen of the oligonucleotide substrate and the 3′- and 2′-moieties of the guanosine nucleophile, are mediated by three distinct metal ions. This approach provides a general tool for distinguishing active site metal ions and allows the properties and roles of individual metal ions to be probed, even within the sea of metal ions bound to RNA.

Divalent metal ions play a critical role in catalysis by many RNA and protein enzymes (e.g., see refs. 1–10). Determining the number of metal ions in an enzymatic active site and delineating their catalytic roles are crucial for elucidating the catalytic mechanisms of these enzymes (e.g., refs. 1–3, 5, 9, and 11–34). This presents a formidable challenge, especially for RNA enzymes, as the metal ions that directly participate in the chemical transformation are bound within a sea of metal ions that coat the charged RNA backbone and facilitate RNA folding (Fig. 1; e.g., see refs. 32–39).

The *Tetrahymena* group I ribozyme (E) derived from a self-splicing group I intron catalyzes a reaction that mimics the first step of splicing, in which an exogenous guanosine nucleophile (G) cleaves a specific phosphodiester bond of an oligonucleotide substrate (S; Eq. **1**; refs. 40–42).

$$\overset{-5}{C}\,C\,C\,U\,\overset{-3}{C}\,U\overset{-1}{p}A + G_{OH} \xrightarrow{E} C\,C\,C\,U\,C\,U_{OH} + GpA \quad [1]$$

Three metal ion interactions contribute to catalysis by this ribozyme (Fig. 2). These interactions were previously identified by modification of specific substrate atoms that alter metal ion specificity; reactions with sulfur- or nitrogen-substituted substrates were severely compromised in Mg^{2+} but were stimulated by addition of softer metal ions such as Mn^{2+} (3, 5, 7, 9). A fundamental question that remains unanswered, however, is whether these interactions are mediated by the same or by distinct metal ions.

We report here the development of an approach that combines atomic-level substrate modifications with quantitative analyses to determine the affinity of individual metal ions for an enzymatic active site. These affinities provide a fingerprint for each metal ion, allowing distinct metal ions to be distinguished. Using this approach, we have provided evidence for three distinct metal ions within the active site of the *Tetrahymena* ribozyme. The results and the approach described herein will allow us to further probe the functional consequences of specific metal ion interactions and the catalytic role of individual metal ions, even within the sea of metal ions bound to RNA.

Materials and Methods

Materials. Ribozyme was prepared by *in vitro* transcription with T7 RNA polymerase as described (43). Oligonucleotides with 3′-thio modifications were prepared by using a published procedure (44). Oligonucleotide substrates were 5′-end-labeled with [γ-^{32}P]ATP and purified as described previously (43, 45).

General Kinetic Methods. All reactions were single-turnover, with ribozyme in excess of labeled oligonucleotide substrate, and were carried out at 30°C in 50 mM buffer and 10 mM $MgCl_2$ unless otherwise specified (7, 40, 41, 46). The buffers used were NaMes (pH 6.3–7.0) and NaEPPS (pH 7.1–8.5) [EPPS is *N*-(2-hydroxyethyl)piperazine-*N*′-(3-propanesulfonic acid)]. Reactions were followed by polyacrylamide gel electrophoresis and were analyzed as described (40, 45).

Determination of Rate and Equilibrium Constants. $(k_c/K_m)^{G_X}$ is the second-order rate constant for the reaction E·S + $G_X \rightarrow$ products (G_X = G or G_{NH_2}), and was determined for the oligonucleotide substrates $S_{3'S}$ and $S_{3'O}$ (see Scheme 1 in *Results*). Values of $(k_c/K_m)^{G_X}$ were determined at pH 7.9, with E saturating with respect to S (50–200 nM E, $K_d^S \approx 1$ nM) and with subsaturating G_X (10–50 μM G_X, $K_d^G = 360$ μM; $K_d^{G_{NH_2}} \geq 110$ μM).

$(k_c/K_m)^{G_{3'X}U}$ is the second-order rate constant for the reverse reaction: E·P + $G_{3'X}U \rightarrow$ E·S + $G_{3'XH}$ (X = S or O). Values of $(k_c/K_m)^{G_{3'X}U}$ were determined at pH 6.3, with trace amounts of 5′-labeled $G_{3'X}U$ (<0.1 nM) and E·P subsaturating with respect to $G_{3'X}U$ [0.2–10 μM E·P; $K_d^{GpU} \geq 300$ μM (47)].

Equilibrium dissociation constants of $S_{3'S}$ and P were determined by pulse–chase experiments and inhibition methods, respectively, as described (7, 40, 48).

Data Analysis. The Mn^{2+} concentration dependences for rescue of the reaction of the individual modified substrates were analyzed according to the model of Fig. 3*A* described in *Results*. The data were fit to Eq. **3**, derived from Fig. 3*A*, to obtain the affinity of the Mn^{2+} ion responsible for rescuing the reaction of the individual modified substrates (see *Results*).

The Mn^{2+} concentration dependence of the reaction of $S_{3'S}$ with G_{NH_2} was fit to Eq. **2**,

$$k_{obsd}^{rel} = k_o^{rel}\left(1 + \frac{K^{Mn_A} + a[Mn^{2+}]}{K^{Mn_A} + [Mn^{2+}]}\right)\left(1 + \frac{K^{Mn_C} + b[Mn^{2+}]}{K^{Mn_C} + [Mn^{2+}]}\right), \quad [2]$$

Abbreviations: E refers to the *Tetrahymena* ribozyme; S and P refer to the oligonucleotide substrate and product with the sequence CCCUCUA and CCCUCU, respectively, without specification of the substitutions. $S_{3'S}$ and $S_{3'O}$ refer to oligonucleotide substrates with a 3′-sulfur and 3′-oxygen leaving group, respectively, as defined in the text; G and G_{NH_2} refer to the guanosine nucleophiles with a 2′-OH and 2′-NH_2 group, respectively; $G_{3'S}U$ and $G_{3'O}U$ refer to GpU dinucleotides with a 3′-sulfur and 3′-oxygen at the G residue, respectively. P1 is the duplex formed between S or P and the internal guide sequence (IGS) of E. $(E{\cdot}S)_o$ and $(E{\cdot}S)_c$ refer to the open and closed ribozyme·substrate complexes, respectively (see Scheme 2).

§To whom reprint requests may be addressed: E-mail: herschla@cmgm.stanford.edu or jpicciri@midway.uchicago.edu.

The publication costs of this article were defrayed in part by page charge payment. This article must therefore be hereby marked "*advertisement*" in accordance with 18 U.S.C. §1734 solely to indicate this fact.

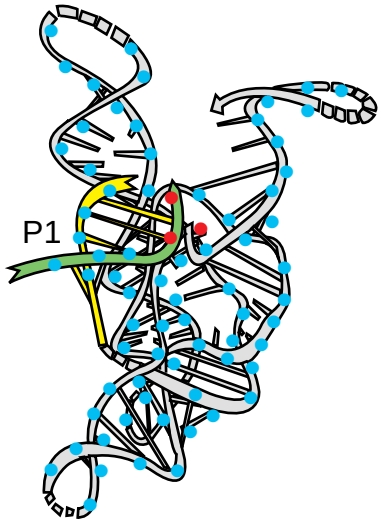

Fig. 1. Catalytic metal ions are bound within a sea of metal ions that coat RNA. A three-dimensional model for the *Tetrahymena* ribozyme complexed with the oligonucleotide substrate is depicted, with the oligonucleotide substrate (S) shown in green, the internal guide sequence (IGS) of the ribozyme in yellow, and the rest of the ribozyme in light gray. P1 is the duplex formed between S or P and the IGS. The blue dots depict the numerous metal ions that coat the RNA backbone; this ribozyme, which contains ~400 nucleotides, is expected to bind 100–200 divalent metal ions (33, 68–70). The red dots depict specific active site metal ions that directly participate in the chemical reaction, which are the focus of this investigation. Adapted from an original drawing by L. Jaeger.

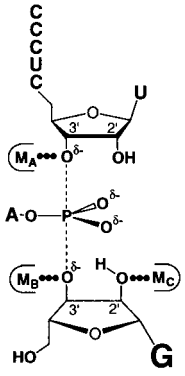

Fig. 2. Metal ion interactions in the transition state of the *Tetrahymena* ribozyme reaction (3, 5, 7, 9). The dashed lines depict the partial bonds between the 3′-oxygen of S and the 3′-oxygen of G to the reactive phosphorus. δ− depicts the partial negative charge on the 3′-oxyanions of S and G and on the nonbridging oxygens of the reactive phosphoryl group. The thin outline represents the metal ion binding site formed by the ribozyme. M_A is the metal ion interacting with the 3′-atom of S (3), M_B is the metal ion interacting with the 3′-moiety of G (9), and M_C is the metal ion interacting with the 2′-moiety of G (5, 7). The results presented herein suggest that these ligands interact with three distinct metal ions.

in which K^{Mn_A} and K^{Mn_C} are the affinities of Mn^{2+}_A and Mn^{2+}_C, respectively, and were fixed at values determined from independent experiments with single modifications (0.8 mM and 0.3 mM, respectively). The rate enhancement provided by the rescuing Mn^{2+}_A is specified by a ($a = k^{rel}_{Mn_A}/k^{rel}_{Mg_A}$, $k^{rel} = k^{S_{3'}S}/k^{S_{3'}O}$). Analogously, b is the rate enhancement provided by the rescuing Mn^{2+}_C, with $b = k^{rel}_{Mn_C}/k^{rel}_{Mg_C}$ and $k^{rel} = k^{G_{NH_2}}/k^{G}$. Values of a and b were fixed at $a = 100$ and $b = 20$, determined in independent experiments with single modifications ($S_{3'}S$ or G_{NH_2}).

Eqs. **2** and **3** assume that the Mn^{2+} rescuing the modified substrate is independent of the Mn^{2+} affecting the reactivity of the unmodified substrate and has no effect on the reactivity of the unmodified substrate. These assumptions are supported by independent experiments (see text and legend of Figs. 4 and 6). The good fits of the data in Figs. 4*B*, 5*B*, and 6*B* to Eqs. **2** and **3** are also consistent with these assumptions.

Results and Discussion

We first describe the general approach for determining metal ion affinities, highlighting critical features of the experimental design. The subsequent sections then apply this approach to determine and distinguish between active site metal ions in the *Tetrahymena* ribozyme. The same approach can be used to distinguish active site metal ions in other RNA and protein enzymes.

General Approach to Obtain Affinities of Active Site Metal Ions. Quantitative analysis of the effect of Mn^{2+} on the reactivity of a modified substrate allows determination of the affinity of a rescuing Mn^{2+}. This affinity can then be compared to the affinities of Mn^{2+} ions that rescue substrates with modifications at different positions. The finding of identical Mn^{2+} affinities would be consistent with rescue by a common metal ion, whereas different affinities would demonstrate rescue by distinct metal ions.

Fig. 3 illustrates this approach for the example of $S_{3'}S$, in which the 3′-bridging oxygen of the oligonucleotide substrate is replaced by sulfur. With Mg^{2+} bound at metal site A, the reaction rate of $S_{3'}S$ is slow relative to the unmodified substrate $S_{3'}O$ (k^{rel}_{Mg}), but this relative reactivity is stimulated when Mn^{2+} replaces Mg^{2+} at site A (k^{rel}_{Mn}). Thus, k^{rel}_{Mn} is greater than k^{rel}_{Mg} in Fig. 3*A*. Fig. 3*B* shows the expected dependence of the observed relative rate constant, k^{rel}_{obsd}, on the concentration of added Mn^{2+}. k^{rel}_{obsd} depends on the fraction of ribozyme with bound Mn^{2+} (^{Mn}E), as described by Eq. **3a**. As the fraction of ^{Mn}E is a function of K^{Mn}, the affinity of Mn^{2+} for the *free* ribozyme, the value of K^{Mn} can be determined from the dependence of k^{rel}_{obsd} on Mn^{2+} concentration, as described by Eq. **3b**. The Mn^{2+} affinity provides a distinct physical constant that can be used to distinguish this rescuing metal ion from other metal ions.

$$k^{rel}_{obsd} = k^{rel}_{Mg} \times \{\text{fraction } ^{Mg}\text{E}\} + k^{rel}_{Mn} \times \{\text{fraction } ^{Mn}\text{E}\} \quad \textbf{[3a]}$$

$$k^{rel}_{obsd} = k^{rel}_{Mg} \times \frac{K^{Mn}}{[Mn^{2+}] + K^{Mn}} + k^{rel}_{Mn} \times \frac{[Mn^{2+}]}{[Mn^{2+}] + K^{Mn}}. \quad \textbf{[3b]}$$

Two features are crucial for the determination and comparison of Mn^{2+} affinities. First, in addition to the effect of the specific Mn^{2+} that rescues reaction of the modified substrate, Mn^{2+} can also have nonspecific effects by binding to other metal ion sites; this is illustrated by the Mn^{2+} occupancy of metal sites B and C in Fig. 3*A*. To minimize Mn^{2+} occupancy at other sites as well as to ensure folding of the ribozyme, a constant background of 10 mM Mg^{2+} was used in the experiments described herein. Even with this precaution, it remains necessary to use the relative rate constants, k^{rel}, to control for nonspecific Mn^{2+} effects and to isolate the effect of the specific rescuing Mn^{2+} (see ref. 7 for detailed description). Second, to compare the Mn^{2+} affinities obtained from different substrate modifications, it is critical to obtain an affinity of the rescuing Mn^{2+} that is *not* perturbed by the modification. Therefore, the rescue is carried out under conditions such that the substrate bearing the modification is not bound within the active site in the starting ground state. If the starting ground state is the free ribozyme as in Fig. 3*A* (^{Mg}E and ^{Mn}E), then the K^{Mn} obtained reflects the Mn^{2+} affinity for the free ribozyme. This affinity is independent of the substrate modification because in this ground state, the substrate is not bound in the active site such that the metal ion does not interact with the modified group. Rescue occurs through the interaction of Mn^{2+} with the modified group in the transition state (Fig. 3*A*, $[^{Mg}E^{\cdot S}_{G}]^{\ddagger}$ and $[^{Mn}E^{\cdot S}_{G}]^{\ddagger}$). As the transition state is formed only transiently, this metal ion interaction does not affect the observed Mn^{2+} affinity. In some experiments below, it is more convenient to determine the Mn^{2+} affinities with bound substrates; the affinity of Mn^{2+} for free E can be obtained from these Mn^{2+} affinities and the independently determined Mn^{2+} effect on substrate binding affinities according to simple thermodynamic cycles (see below).

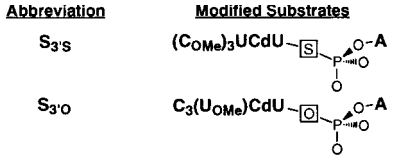

Scheme 1.¶

Determination of the Affinity of the Mn^{2+} That Interacts with the 3′-Leaving Group of S. The metal ion interaction with the 3′-oxygen of S (Fig. 2, M_A) was probed by replacing this oxygen with sulfur (Fig. 3*A* and Scheme 1, $S_{3'S}$). Previous work showed that the oligonucleotide substrate binds the ribozyme in two steps (Scheme 2). First, the open complex, $(E{\cdot}S)_o$, forms, in which S binds solely by base-pairing interactions with the IGS of the ribozyme to form the P1 duplex (49–52). Second, the P1 duplex docks into the active site via tertiary interactions to form the closed complex, $(E{\cdot}S)_c$ (45, 49, and 51–57). To obtain a Mn^{2+} affinity for metal site A that is unperturbed by the modified substrate, the $(E{\cdot}S)_o$ complex can be used as the starting ground state because S does not interact with active site residues and bound metal ions in the open complex (Scheme 2).‖

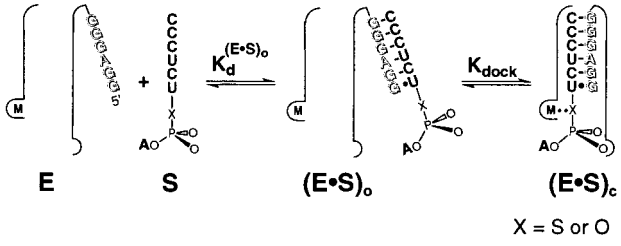

Scheme 2.

The affinity of $S_{3'S}$ and additional observations indicate that $S_{3'S}$ binds E in predominantly the $(E{\cdot}S)_o$ complex (i.e., $K_{dock} < 1$ for $S_{3'S}$; 30°C, 2–100 mM Mg^{2+} and 0–20 mM Mn^{2+}/10 mM Mg^{2+}; unpublished results). In contrast, the standard unmodified substrate binds E to form a stable $(E{\cdot}S)_c$ complex. We therefore introduced a 2′-methoxy (OMe) group at the U(−3) residue of $S_{3'O}$ (Scheme 1), a modification that causes $S_{3'O}$ to also bind predominantly in the open complex, analogous to $S_{3'S}$, but has no effect on other reaction steps (49, 51–54). This allows the effects of Mn^{2+} on the same reaction steps, that of $(E{\cdot}S)_o$ + G → products $[(k_c/K_m)^G$, Fig. 4], to be monitored for both $S_{3'S}$ and $S_{3'O}$. This is also critical for interpretation of rescue experiments.

Mn^{2+} increases the rate of reaction of $S_{3'S}$ 10^4-fold, whereas the effect on the reactivity of $S_{3'O}$ is only 40-fold (Fig. 4*A*, closed vs. open circles). As the effects of Mn^{2+} on the reactivity of $S_{3'O}$ and $S_{3'S}$ are similar above 1 mM Mn^{2+}, the rescue is achieved at lower Mn^{2+} concentrations, suggesting that the reaction of $S_{3'S}$ is rescued by a Mn^{2+} ion(s) distinct from the Mn^{2+} affecting the reactivity of $S_{3'O}$. The effect of Mn^{2+} specific to $S_{3'S}$ was isolated by plotting the reactivity of $S_{3'S}$ relative to $S_{3'O}$, k^{rel} (Fig. 4*B*, closed circles). This Mn^{2+} concentration dependence of k^{rel}

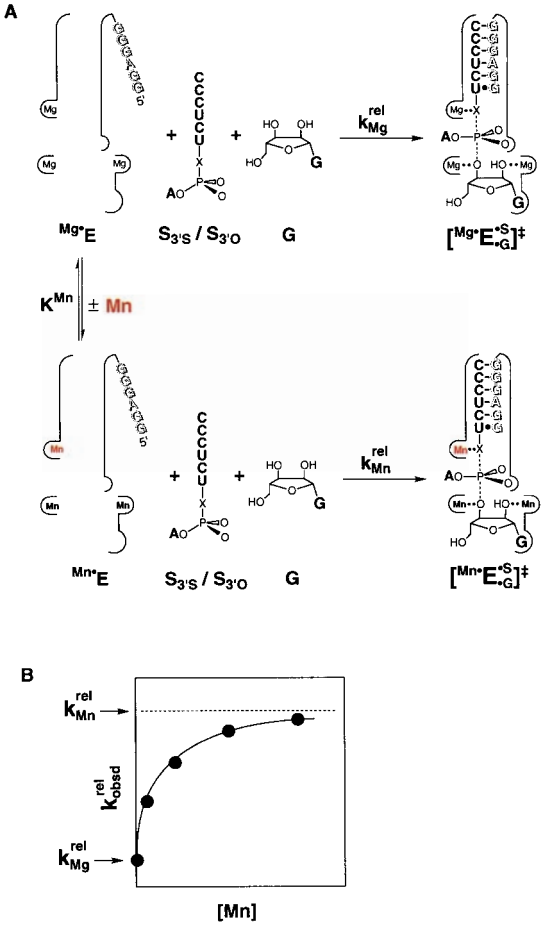

Fig. 3. Schematic description of the method for determining the affinities of rescuing metal ions. (*A*) Equilibrium for binding of Mn^{2+} (red) to metal site A in the free ribozyme (K^{Mn}), and reaction of $S_{3'S}$ and $S_{3'O}$ with Mg^{2+} and Mn^{2+} bound at site A, with relative rate constants of k^{rel}_{Mg} and k^{rel}_{Mn}, respectively ($k^{rel} = k^{S3'S}/k^{S3'O}$). The ribozyme active site is schematically represented by the thin outline, with the IGS of the ribozyme shown by shaded letters. Addition of Mn^{2+} would lead to partial occupancy of all metal ion sites, depending on the metal ion concentration and the Mn^{2+} affinity of each site. This is represented by the Mn^{2+} occupancy of metal sites B and C in the ^{Mn}E and $[^{Mn}E^{S}_{G}]^{‡}$ species. (*B*) The Mn^{2+} concentration dependence of the observed reactivity of $S_{3'S}$ relative to $S_{3'O}$ (k^{rel}_{obsd}) predicted from the model of *A*. Analysis of the Mn^{2+} concentration dependence gives the Mn^{2+} affinity for metal site A in the free ribozyme, as described in the text.

suggests that a single rescuing Mn^{2+} binds to the $(E{\cdot}S)_o$ complex with a dissociation constant of $K^{Mn_A} = 0.8 \pm 0.2$ mM (Fig. 4*B* and Eq. **3b**).

Additional experiments indicated that the affinity of $S_{3'S}$ is the same, within error, in the presence or absence of added Mn^{2+} (dissociation constants for $S_{3'S}$ of 0.6 ± 0.1, 0.4 ± 0.1, and 0.6 ± 0.1 nM were obtained with 0, 5, and 20 mM Mn^{2+}; 30°C, 10 mM Mg^{2+}; unpublished results). The absence of a Mn^{2+} effect on the affinity of $S_{3'S}$ indicates that the affinity of bound Mn^{2+} is not affected by bound $S_{3'S}$ either, according to the thermodynamic cycle of Eq. **4** ($K^{Mn}_{E{\cdot}S_{3'S}}/K^{Mn}_{E} = K^{S_{3'S}}_{d,Mn}/K^{S_{3'S}}_{d,Mg} = 1$). This is consistent with the expectation described above that Mn^{2+} would bind to free E with the same affinity as it binds to the $(E{\cdot}S)_o$ complex because of the absence of interactions of S with the active site in the open complex (Scheme 2). The value of K^{Mn_A} thus represents the unperturbed affinity of Mn^{2+} for metal site A in the free ribozyme. This provides a quantitative physical constant that can be used to identify M_A, the metal ion that interacts with the 3′-atom of S.

¶2′-OMe groups were introduced into the −4 to −6 residues of $S_{3'S}$ (Scheme 1); the sole effect of this modification is to prevent miscleavage of $S_{3'S}$, allowing more accurate determination of reaction rates (49, 52, 54).

‖The $(E{\cdot}S)_o$ complex, rather than free E, was used as the starting ground state to obtain reaction rates fast enough to be accurately determined. The Mn^{2+} affinity obtained for $(E{\cdot}S)_o$ is expected to be equal to that for free E, as S does not interact with the active site in the open complex (see text). This expectation was confirmed by the absence of a Mn^{2+} effect on formation of the open complex described later in the text.

$$\begin{array}{ccc} E^{\bullet Mg} + S_{3'S} & \underset{K_{d,Mg}^{S_{3'S}}}{\rightleftharpoons} & (E^{\bullet Mg}_{\bullet S_{3'S}})_o \\ K_E^{Mn} \Big\downarrow \Big\uparrow \pm Mn & & K_{E\bullet S_{3'S}}^{Mn} \Big\downarrow \Big\uparrow \pm Mn \\ E^{\bullet Mn} + S_{3'S} & \underset{K_{d,Mn}^{S_{3'S}}}{\rightleftharpoons} & (E^{\bullet Mn}_{\bullet S_{3'S}})_o \end{array} \quad [4]$$

The 2′-Moiety of G and the 3′-Leaving Group of S Interact with Two Distinct Metal Ions. To determine whether M_A is the same or distinct from other active site metal ions, we compared the affinity of Mn_A^{2+} with those of the Mn^{2+} ion(s) that interact with the other ligands (Fig. 2; refs. 5, 7, and 9). A metal ion interaction with the 2′-moiety of G (Fig. 2, M_C) was identified in group I introns by using 2′-aminoguanosine (G_{NH_2}; refs. 5 and 7), and the affinity of the Mn^{2+} that interacts with G_{NH_2} was determined by experiments analogous to those described above (7). These studies indicated that Mn_C^{2+} binds to free E with a dissociation constant of $K^{Mn_C} = 0.28 \pm 0.06$ mM (Fig. 4*B*, open symbols, 10 mM Mg^{2+}; ref. 7). As described above, this affinity (K^{Mn_C}) is unperturbed by modification on the 2′-moiety of G, because the G site is unoccupied in the free ribozyme (Fig. 3*A*). Thus, the stronger binding of Mn_C^{2+} than Mn_A^{2+} to the free ribozyme suggests that the 3′-atom of S and the 2′-moiety of G interact with two distinct metal ions (Fig. 4*B*, open vs. closed symbols).

As the difference in the affinities of Mn_C^{2+} and Mn_A^{2+} is small, we tested this conclusion by determining the number of metal ions required to rescue the reaction of $S_{3'S}$ with G_{NH_2}. Mn^{2+} increases the rate of reaction of G_{NH_2} with $S_{3'S}$ more than the reaction of G with $S_{3'S}$ (Fig. 5*A*, closed squares vs. circles). To isolate the effects of Mn^{2+} specific to modifications on $S_{3'S}$ and G_{NH_2}, the rate of reaction of $S_{3'S}$ with G_{NH_2} relative to the reaction of $S_{3'O}$ with G was plotted (Fig. 5*B*; k^{rel}). The Mn^{2+} concentration dependence of k^{rel} is steeper than predicted for a single rescuing Mn^{2+} (Fig. 5*B*, data points vs. dashed curve). The solid line in Fig. 5*B* shows the Mn^{2+} concentration dependence *predicted* for rescue by Mn_A^{2+} and Mn_C^{2+} with affinities of 0.8 and 0.3 mM and rate enhancements of 100- and 20-fold, respectively (Eq. **2**), the Mn^{2+} affinities and rate enhancements observed in the aforementioned experiments with single substitutions (Fig. 4 and ref. 7). The good fit of the predicted concentration dependence to the observed data provides strong independent support for the conclusion that M_A and M_C are distinct.

The 3′-Moiety of G Interacts with a Third Metal Ion. Finally, we measured the affinity of the Mn^{2+} that interacts with the 3′-moiety of G (Fig. 2, M_B; ref. 9). The 3′-oxygen of the guanosine of GpU was replaced with sulfur ($G_{3'O}U \rightarrow G_{3'S}U$), and the reverse reaction was followed, in which the oligonucleotide product (P) attacks GpU to regenerate S and G (CCCU-CU_{OH} + GpU → CCCUCUpU + G_{OH}). To obtain the affinity of Mn_B^{2+} for the E·P complex, the experiment was carried out with E·P subsaturating with respect to $G_{3'S}U$ or $G_{3'O}U$ to follow the reaction: $E{\cdot}P + G_{3'X}U \rightarrow E{\cdot}S + G_{3'XH}$ [$(k_c/K_m)^{G_{3'X}U}$, X = O or S; Fig. 6*A*]. As the G site is unoccupied in the E·P complex, the obtained Mn_B^{2+} affinity (K^{Mn_B}) is not perturbed by the modification on the 3′-moiety of G (cf. Fig. 3*A*).

The rate of reaction of $G_{3'S}U$ increases 2000-fold, whereas the rate of reaction of $G_{3'O}U$ increases only 60-fold (10 mM Mg^{2+}; Fig. 6*A*). Following the approach described above, the Mn^{2+} effect specific to $G_{3'S}U$ was analyzed from the relative reactivity (Fig. 6*B*, k^{rel}). The Mn^{2+} concentration dependence of k^{rel} suggests that a single rescuing Mn^{2+} (Mn_B^{2+}) binds to the E·P complex with a dissociation constant of $K^{Mn_B} = 7 \pm 1$ mM (Fig. 6*B*, solid line; Eq. **3b**). In contrast, Mn_C^{2+}, which interacts with the 2′-moiety of G, binds to E·P 40-fold stronger, with $K^{Mn_C} = 0.19 \pm 0.04$ mM (Fig. 6*B*, dashed line; ref. 7). As described above, the affinity of Mn_C^{2+} for E·P is not perturbed by the modification on the 2′-moiety of G. The distinct affinities of Mn_B^{2+} and Mn_C^{2+} for

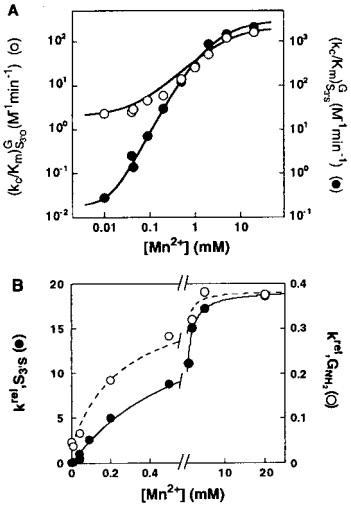

Fig. 4. Mn^{2+} rescues the reactivity of $S_{3'S}$. (*A*) Effect of Mn^{2+} on the rate of reaction $(E{\cdot}S)_o + G \rightarrow$ products [$(k_c/K_m)^G$] with $S_{3'S}$ (●) and $S_{3'O}$ (○), determined as described in *Materials and Methods*. The effect of Mn^{2+} on the reaction of $S_{3'O}$ arises from a Mn^{2+} interacting with the A(+1) residue that is distinct from the Mn^{2+} that specifically rescues $S_{3'S}$ (unpublished results). (*B*) The effect of Mn^{2+} on the reactivity of $S_{3'S}$ relative to $S_{3'O}$ [●, $k^{rel} = (k_c/K_m)^G_{S_{3'S}}/(k_c/K_m)^G_{S_{3'O}}$]. The line is a fit of the Mn^{2+} concentration dependence of k^{rel} values to Eq. **3b**, derived from the model of Fig. 3*A*, and gives $K^{Mn_A} = 0.8 \pm 0.2$ mM. The Mn^{2+} concentration dependence of the relative reactivity of G_{NH_2} (○) is from ref. 7 and is shown for comparison.

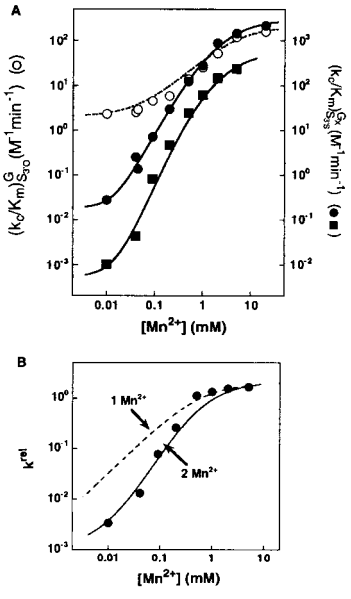

Fig. 5. Two Mn^{2+} ions are required to rescue the reaction of $S_{3'S}$ with G_{NH_2}. (*A*) Effect of Mn^{2+} on the reaction $E{\cdot}S + G_X \rightarrow$ products [$(k_c/K_m)^{G_X}$; G_X = G or G_{NH_2}] with $S_{3'O}$ and G (○), $S_{3'S}$ and G (●), and $S_{3'S}$ and G_{NH_2} (■). Determined as in Fig. 4 with subsaturating G_X. The data for reactions of $S_{3'O}$ with G and of $S_{3'S}$ with G are from Fig. 4*A* and are shown for comparison. (*B*) The effect of Mn^{2+} on the rate of reaction of $S_{3'S}$ with G_{NH_2} relative to that of $S_{3'O}$ with G [$k^{rel} = (k_c/K_m)^{G_{NH_2}}_{S_{3'S}}/(k_c/K_m)^G_{S_{3'O}}$]. The solid line is the Mn^{2+} concentration dependence of the relative reactivity *predicted* from a model in which two Mn^{2+} ions, Mn_A^{2+} and Mn_C^{2+}, independently rescue the reaction of $S_{3'S}$ and G_{NH_2}, respectively (see Eq. **2**). The dashed line is the best fit of data to a model in which a single Mn^{2+} ion rescues the reaction of $S_{3'S}$ with G_{NH_2}.

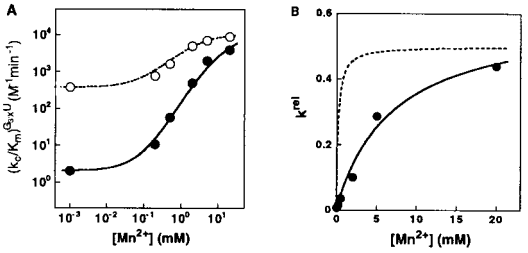

Fig. 6. Mn^{2+} rescues the reactivity of $G_{3'S}U$. (*A*) Effect of Mn^{2+} on the rate of the reverse reaction E·P + $G_{3'X}U \rightarrow$ E·S + $G_{3'XH}$ [$(k_c/K_m)^{G3'XU}$] with $G_{3'S}U$ (●) and $G_{3'O}U$ (○), determined as described in *Materials and Methods*. The effect of Mn^{2+} on the reaction of $G_{3'O}U$ arises from a Mn^{2+} distinct from the Mn^{2+} ions investigated herein (unpublished results). (*B*) The effect of Mn^{2+} on the reactivity of $G_{3'S}U$ relative to $G_{3'O}U$ [$k^{rel} = (k_c/K_m)^{G3'SU}/(k_c/K_m)^{G3'OU}$]. The solid line is a fit of the data to Eq. **3b**, derived from the model of Fig. 3*A*, and gives $K^{Mn_B} = 7 \pm 1$ mM. The dashed line is a hypothetical Mn^{2+} concentration dependence of k^{rel} expected if Mn_C^{2+}, which binds to E·P with a dissociation constant of 0.19 mM (7), were responsible for rescue of $G_{3'S}U$.

E·P thus strongly suggest that the 2′- and 3′-moieties of G interact with two distinct metal ions.

Independent experiments showed that Mn^{2+} at concentrations up to 10 mM has less than a 2-fold effect on binding of P to E (10 mM Mg^{2+}). This observation and thermodynamic analysis analogous to that described above in Eq. **4** indicate that Mn_B^{2+} binds to free E with $K^{Mn_B} = 7$ mM, the same as that determined for E·P above. Thus, the binding affinities of Mn_A^{2+} and Mn_B^{2+} for free E differ by 10-fold, strongly suggesting that they are distinct.

The effect of Mg^{2+} on the binding of Mn^{2+} to each metal site provided additional evidence that Mn_B^{2+} is distinct from Mn_A^{2+} and Mn_C^{2+}. The affinity of each Mn^{2+} for free E was determined at a series of Mg^{2+} concentrations in experiments analogous to those described above. The dissociation constants of Mn_A^{2+} and Mn_C^{2+} increase linearly with increasing Mg^{2+} above 2 mM Mg^{2+} (Table 1), suggesting that Mn^{2+} competes with a Mg^{2+} at sites A and C. In contrast, the affinity of Mn_B^{2+} remains the same at 2 and 10 mM Mg^{2+} and weakens only above 10 mM Mg^{2+}. These results provide further evidence that M_B is distinct from M_A and M_C.

The 2′-OH of U(−1), which precedes the cleavage site (Eq. **1**), contributes 10^3-fold in the chemical step (45, 58) and has been suggested to interact with a metal ion (5, 59). However, results with this 2′-OH replaced by an amino group suggest that there is no direct metal ion coordination with this group (60). Instead, the 2′-OH of U(−1) appears to hydrogen bond to the 3′-oxygen of S to help stabilize the oxyanion in the transition state (Fig. 7; refs. 54, 58, 60, and 61). The absence of a metal ion interaction with the U(−1) 2′-OH presumably explains why substituting a 2′-H for the 2′-OH of G has a larger deleterious effect than for the 2′-OH of U(−1) (>10^6- vs. 10^3-fold; refs. 58, 62, and 63 and S. Shan and D.H., unpublished results), as placing a hydrogen atom adjacent to a metal ion is likely to be energetically very costly.

Table 1. Effect of Mg^{2+} on the affinity of rescuing Mn^{2+} ions

	$K^{Mn,app}$,* mM		
[Mg^{2+}], mM	Mn_A^{2+}	Mn_B^{2+}	Mn_C^{2+}
2	0.16	5	0.058
10	0.82	7	0.28
50	—	13	1.3
100	6.3	—	—

*The observed dissociation constant of Mn^{2+} from free E at each Mg^{2+} concentration was determined in experiments analogous to those described in the text with 10 mM Mg^{2+}. The dissociation constants of Mn_C^{2+} are from ref. 7. As described in the text, the measurements were made with $(E{\cdot}S)_o$ or E·P, and the absence of a Mn^{2+} effect on formation of $(E{\cdot}S)_o$ and E·P suggests that the same Mn^{2+} affinities hold for free E. This was directly verified in several instances (ref. 7 and unpublished results). The dissociation constants for Mn_A^{2+} and Mn_C^{2+} were determined at pH 7.9, and those for Mn_B^{2+} were determined at pH 6.3 (see text and refs. 7 and 66). The Mn^{2+} dissociation constants obtained have been shown to be unaffected by the following changes in pH: Mn_A^{2+}, pH 7.0–7.9; Mn_B^{2+}, pH 6.3–7.1; Mn_C^{2+}, pH 5.0–7.9 (refs. 7 and 66 and unpublished results), as expected because RNA functional groups typically have pK_a values ≥9 or ≤4. The error associated with each $K^{Mn,app}$ value is less than ±30%, and specific error limits for the apparent Mn^{2+} affinities at 10 mM Mg^{2+} are in the text.

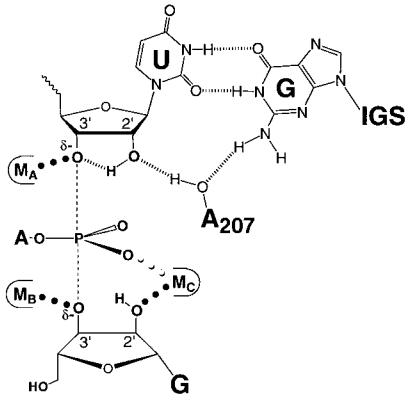

Fig. 7. Model for transition state interactions within the active site of the *Tetrahymena* ribozyme. The dashed lines (– – –) depict the partial bonds between the reactive phosphorus and the 3′-oxygens of G and U(−1), and δ− depict the partial negative charges on the 3′-oxyanions of S and G, as described in the legend to Fig. 2. Experimental observations from this and previous work have provided evidence for the active site interactions depicted by ••• and ⁞⁞⁞ as described in the text. The results described herein strongly suggest the presence of at least three distinct metal ions at the ribozyme active site (M_A, M_B, and M_C; refs. 3, 5, 7, and 9 and this work).

Conclusions and Implications

The results of this study provide strong evidence that the *Tetrahymena* ribozyme active site contains three distinct metal ions that interact with the 3′-atom of S, the 3′-moiety of G, and the 2′-moiety of G, respectively, in an asymmetric transition state (Figs. 2 and 7). The metal ion interaction with the leaving group of S could contribute to catalysis by stabilizing the developing negative charge on the leaving group and may also contribute by ground state electrostatic destabilization (Fig. 7, M_A; refs. 3 and 64 and unpublished results). This 3′-oxyanion is further stabilized by a hydrogen bond from the neighboring 2′-OH of U(−1) (Fig. 7; ref. 58 and unpublished results), and this 2′-OH may be situated within a network of active site interactions that involves the 2′-OH of A207 and the exocyclic amine of the G·U wobble pair that specifies the cleavage site (Fig. 7; refs. 54, 60, 61, 65, and 66). The metal ion interaction with the 3′-moiety of G is expected to help deprotonate the 3′-OH of G at physiological pH, thereby activating the nucleophile (Fig. 7, M_B; ref. 9). The metal ion that interacts with the 2′-moiety of G may also coordinate to the 3′-OH of G to further aid deprotonation of the 3′-OH (Fig. 7, M_C; refs. 5 and 7); this metal ion may in addition be used to align the reactive phosphoryl group of S and G with respect to one another within the active site, thereby accelerating the reaction (Fig. 7; ref. 7).

The number of catalytic metal ions at RNA and protein active sites has been the subject of much discussion and speculation (e.g., refs. 1, 2, 5, 9, 11–29, 33, and 34). As demonstrated herein, quantitative analysis with modified substrates to obtain thermodynamic fingerprints for specific metal ions provides a powerful tool for identifying and distinguishing active site metal ions. The ability to distinguish between

BIOCHEMISTRY

distinct metal ion sites will help address the number of active site metal ions, the identity of their ligands, and the roles of these metal ions in catalysis by RNA and protein enzymes.

We are grateful to F. Eckstein for the gift of 2′-aminoguanosine, L. Beigelman for oligonucleotides, G. Narlikar for initial results and intellectual input, J. Brauman and members of the Herschlag laboratory for comments on the manuscript, and a reviewer for suggestions on the description of the experimental approach. This work was supported by grants from the National Institutes of Health to D. H. and the Howard Hughes Medical Institute to J.A.P.; S. Sun is a Research Associate of the Howard Hughes Medical Institute.

1. Dismukes, G. C. (1996) *Chem. Rev.* **96**, 2909–2926.
2. Wilcox, D. E. (1996) *Chem. Rev.* **96**, 2435–2458.
3. Piccirilli, J. A., Vyle, J. S., Caruthers, M. H. & Cech, T. R. (1993) *Nature (London)* **361**, 85–88.
4. Scott, E. C. & Uhlenbeck, O. C. (1999) *Nucleic Acids Res.* **27**, 479–484.
5. Sjögren, A.-S., Pettersson, E., Sjöberg, B.-M. & Strömberg, R. (1997) *Nucleic Acids Res.* **25**, 648–653.
6. Sontheimer, E. J., Sun, S. & Piccirilli, J. (1997) *Nature (London)* **388**, 801–805.
7. Shan, S. & Herschlag, D. (1999) *Biochemistry* **38,** 10958–10975.
8. Warnecke, J. M., Furste, J. P., Hardt, W.-D., Erdmann, V. A. & Hartmann, R. K. (1996) *Proc. Natl. Acad. Sci. USA* **93**, 8924–8928.
9. Weinstein, L. B., Jones, B. C., Cosstick, R. & Cech, T. R. (1997) *Nature (London)* **388**, 805–808.
10. Chen, Y., Li, X. & Gegenheimer, P. (1997) *Biochemistry* **36**, 2425–2438.
11. Steitz, T. A. (1998) *Nature (London)* **391**, 231–232.
12. Black, C. B. & Cowan, J. A. (1998) *J. Biol. Inorg. Chem.* **2**, 292–299.
13. Cowan, J. A. (1997) *J. Biol. Inorg. Chem.* **2**, 168–176.
14. Bujacz, G., Jaskolski, M., Alexandratos, J., Wlodawer, A., Merkel, G., Katz, R. A. & Skalka, A. M. (1996) *Structure* **15**, 89–96.
15. Keck, J. L., Goedken, E. R. & Marqusee, S. (1998) *J. Biol. Chem.* **273**, 34128–34133.
16. Zhang, E., Hatada, M., Brewer, J. M. & Lebioda, L. (1994) *Biochemistry* **33**, 6295–6300.
17. Wedekind, J. E., Poyner, R. R., Reed, G. H. & Rayment, I. (1994) *Biochemistry* **33**, 9333–9342.
18. Duquerroy, S., Camus, C. & Janin, J. (1995) *Biochemistry* **34**, 12513–12523.
19. Kostrewa, D. & Winkler, F. K. (1995) *Biochemistry* **34**, 683–696.
20. Groll, D. H., Jeltch, A., Selent, U. & Pingoud, A. (1997) *Biochemistry* **36**, 11389–11401.
21. Horton, N. C., Newberry, K. J. & Perona, J. J. (1998) *Proc. Natl. Acad. Sci. USA* **95**, 13489–13494.
22. Bone, R., Frank, L., Springer, J. P. & Atack, J. R. (1994) *Biochemistry* **33**, 9468–9476.
23. Zhang, Y., Liang, J.-Y., Huang, S., Ke, H. & Lipscomb, W. N. (1993) *Biochemistry* **32**, 1844–1857.
24. Steitz, T. A. & Steitz, J. A. (1993) *Proc. Natl. Acad. USA* **90**, 6498–6502.
25. Smith, D. & Pace, N. R. (1993) *Biochemistry* **32**, 5273–5281.
26. Kuimelis, R. G. & McLaughlin, L. W. (1996) *Biochemistry* **35**, 5308–5317.
27. Lott, W. B., Pontius, B. W. & von Hippel, P. H. (1998) *Proc. Natl. Acad. Sci. USA* **95**, 542–547.
28. Hermann, T., Auffinger, P., Scott, W. G. & Westhof, E. (1997) *Nucleic Acids Res.* **25**, 3421–3427.
29. Streicher, B., Westhof, E. & Schroeder, R. (1996) *EMBO J.* **15**, 2556–2564.
30. Yarus, M. (1993) *FASEB J.* **7**, 31–39.
31. Pyle, A. M. (1996) in *Metal Ions in Biological Systems*, eds. Sigel, A. & Sigel, H. (Dekker, New York), pp. 479–520.
32. Pan, T., Long, D. M. & Uhlenbeck, O. C. (1993) in *The RNA World*, eds. Gesteland, R. F. & Atkins, J. F. (Cold Spring Harbor Lab. Press, Plainview, NY), pp. 271–302.
33. Beebe, J. A., Kurz, J. C. & Fierke, C. A. (1996) *Biochemistry* **35**, 10493–10505.
34. McConnell, T. S., Herschlag, D. H. & Cech, T. R. (1997) *Biochemistry* **36**, 8293–8303.
35. Draper, D. E. (1996) *Trends Biochem. Sci.* **21**, 145–149.
36. Cate, J. H. & Doudna, J. A. (1996) *Structure* **4**, 1221–1229.
37. Cate, J. H., Hanna, R. L. & Doudna, J. A. (1997) *Nat. Struct. Biol.* **7**, 553–558.
38. Pan, T. (1995) *Biochemistry* **34**, 902–909.
39. Celander, D. W. & Cech, T. R. (1991) *Science* **251**, 401–407.
40. Herschlag, D. & Cech, T. R. (1990) *Biochemistry* **29**, 10159–10171.
41. Herschlag, D. & Cech, T. R. (1990) *Biochemistry* **29**, 10172–10180.
42. Cech, T. R. & Herschlag, D. (1996) in *Nucleic Acids and Molecular Biology*, eds. Eckstein, F. & Lilley, D. M. J. (Springer, Berlin), pp. 1–17.
43. Zaug, A. J., Grosshans, C. A. & Cech, T. R. (1988) *Biochemistry* **27**, 8924–8931.
44. Sun, S., Yoshida, A. & Piccirilli, J. A. (1997) *RNA* **3**, 1352–1363.
45. Herschlag, D., Eckstein, F. & Cech, T. R. (1993) *Biochemistry* **32**, 8299–8311.
46. McConnell, T. S. & Cech, T. R. (1995) *Biochemistry* **34**, 4056–4067.
47. McConnell, T. S. (1995) Ph.D. Thesis (Univ. of Colorado, Boulder).
48. Rose, I. A., O'Connell, E. L., Litwin, S. & Bar Tana, J. (1974) *J. Biol. Chem.* **249**, 5163–5168.
49. Herschlag, D. (1992) *Biochemistry* **31**, 1386–1398.
50. Bevilacqua, P. C., Kierzek, R., Johnson, K. A. & Turner, D. H. (1992) *Science* **258**, 1355–1358.
51. Narlikar, G. J. & Herschlag, D. (1996) *Nat. Struct. Biol.* **3**, 701–710.
52. Narlikar, G. J., Khosla, M., Usman, N. & Herschlag, D. (1997) *Biochemistry* **36**, 2465–2477.
53. Pyle, A. M. & Cech, T. R. (1991) *Nature (London)* **350**, 628–631.
54. Knitt, D. S., Narlikar, G. J. & Herschlag, D. (1994) *Biochemistry* **33**, 13864–13879.
55. Bevilacqua, P. C. & Turner, D. H. (1991) *Biochemistry* **30**, 10632–10640.
56. Strobel, S. A. & Cech, T. R. (1993) *Biochemistry* **32**, 13594–13604.
57. Szewczak, A. A., Ortoleva-Donnelly, L., Ryder, S. P., Moncoeur, E. & Strobel, S. A. (1998) *Nat. Struct. Biol.* **5**, 1037–1042.
58. Herschlag, D., Eckstein, F. & Cech, T. R. (1993) *Biochemistry* **32**, 8312–8321.
59. Sugimoto, N., Tomka, M., Kierzek, R., Bevilacqua, R. C. & Turner, D. H. (1989) *Nucleic Acids Res.* **17**, 355–371.
60. Yoshida, A., Shan, S., Herschlag, D. & Piccirilli, J. A. (1999) *Chem. Biol*., in press.
61. Strobel, S. A. & Ortoleva-Donnelly, L. (1999) *Chem. Biol.* **6**, 153–165.
62. Bass, B. L. & Cech, T. R. (1986) *Biochemistry* **25**, 4473–4477.
63. Tanner, N. K. & Cech, T. R. (1987) *Biochemistry* **26**, 3330–3340.
64. Narlikar, G. J., Gopalakrishnan, V., McConnell, T. S., Usman, N. & Herschlag, D. (1995) *Proc. Natl. Acad. Sci. USA* **92**, 3668–3672.
65. Strobel, S. A. & Cech, T. R. (1995) *Science* **267**, 675–679.
66. Strobel, S. A. & Cech, T. R. (1996) *Biochemistry* **35**, 1201–1211.
67. Shan, S., Narlikar, G. N. & Herschlag, D. (1999) *Biochemistry* **38,** 10976–10988.
68. Quigley, G. J., Teeter, M. M. & Rich, A. (1978) *Proc. Natl. Acad. Sci. USA* **75**, 64–68.
69. Crothers, D. M. (1979) in *Transfer RNA: Structure, Properties, and Recognition*, eds. Schimmel, P. R., Söll, D. & Abelson, J. N. (Cold Spring Harbor Lab. Press, Plainview, NY), pp. 163–176.
70. Bujalowski, W., Graester, E., McLaughlin, L. W. & Porschke, D. (1986) *Biochemistry* **25**, 6365–6371.